VOL. 11, NO. 17, SEPTEMBER 2016 ISSN 1819-6608
ARPN Journal of Engineering and Applied Sciences

www.arpnjournals.com

NUMERICAL PREDICTION OF BRAKE FRICTION PAIR VIBRATION USING DYNAMICS GREEN'S FUNCTION

Muhammad Zahir Hassan[1, 2], Kumaresan Magaswaran[3], Frank Delbressine[1] and Matthias Rauterberg[1]
[1]Department of Industrial Design, Eindhoven University of Technology, The Netherlands
[2]Faculty of Engineering Technology, Universiti Teknikal Malaysia Melaka, Malaysia
[3]School of Engineering, Computing and Built Environment, KDU Penang University College, Malaysia
E-Mail: zahir@utem.edu.my

ABSTRACT

The prediction capability of the brake system vibration is still unable to cover a broad range of frequencies. Current predictive models are contained within a particular range to cater for specific vibration types. Therefore, a numerical model which could make predictions in a broad spectrum range is required. The model presented in this paper is derived with such aim. The model is derived from the interaction between the friction pairs with the focus on the brake pad. The brake disc is simplified as a travelling sinusoidal wave. Where else, the brake pad is modelled as a Euler-Bernoulli beam with forces and distributed friction acting upon it. The Dynamic Green Equation applied in solving the derived friction pair equation. The outcome of the developed model predicted brake pad vibrational frequency coinciding accurately with brake dynamometer experimental results. Therefore, the validated model could be a viable prediction and study tool for various brake system parameters.

Keywords: braking noise, green's function, vibration, modelling.

INTRODUCTION

One of the most important criteria in automotive quality is the vehicle noise, vibration and harshness (NVH). Under the vast umbrella of NVH lies the issue of brake noise and vibration. Even though research of this problem is available in abundance, the predictive capability is still lacking [1]. A complete predictive model will be extremely useful in determining the dynamics of the brake system under various conditions and parameters [2]. Understanding the dynamics enables the engineer to test the desired braking parameters at its limit and identifying its critical limitations [3].

The brake system noise is audibly heard and vibration is physically sensed but both originate from vibrations. Some vibration which is audibly relevant is heard, some are felt and others are ignored by most vehicle passengers. Thus, the study of these phenomena as vibration, in general, gives a wider perspective. This is especially relevant when considering the vibrations of the low-frequency domain which is below 1 kHz. Noise such as groan and roughness and vibrations such as judder and chatter falls within this domain [4]. These vibrations are an intriguing problem as it occurs in a broad spectrum of frequencies thus, it's a challenge predicting these vibrations. Experiments are not deterministic due to the intermittent behaviour of the brake vibrations [5]. May it be the dynamometer experiment or real vehicle testing; repeatability of the results suffers greatly. Nevertheless, desired results are produced but the frequencies of the vibration tend to differ randomly.

The modelling of the brake system is important both as a predictive tool and a guide to understanding its underlying behaviour [1]. A proven model is useful in predicting frequencies of the brakes noise and vibration so that its characteristics can be evaluated early in the design phase itself and amendments could be made before production. The intermittent nature and of the brake noise and vibration demand for a numerical model that is capable of predicting all the frequencies that could occur in the system [6].

A viable brake system model should be derived based on its dynamics. The friction pair of brake pad and brake disc lies at the core of this dynamics. This is so due to the fact that the interaction between the friction pair produces the vibrations during braking [7]. Starting from the brake disc, it is said during vibration it behaves as a travelling sinusoidal wave [8]. Upon contact with the brake pad during braking, this behaviour will greatly influence on the motion of the brake pad. The contact is achieved due to the brake pressure applied by the brake pistons; this applied pressure would cause the brake pad to undergo deformation [9]. The experimental measurement of the brake pad static deformation shows a weakly linear behaviour [10]. A poorly linear means it would follow linear behaviour.

Referring to available literature, the brake system is commonly modelled as lumped rigid model together with other brake system components [11, 12, 13] these types of models studies the brake pad motion constituent of transverse motion or rotational motion or the combined motion of both. The deformation during vibration is neglected. To include deformation an elastic beam model could be adapted in brake system modelling as done by [13, 14]. The brake pad is a complicated element as it experiences multiple forces from various with at least more than one continuous variable. Thus, the partial differentials equations (PDE) are unavoidable in the model.

The PDE is also common in the beam equation. The usage of the dynamic green equation is a common practice in beam modelling [15, 16, 17]. Nevertheless, it is applicable to the brake pad modelling. The available literature shows that the green function is used in conditions where the beam is subjected to a single periodic

load may it be stationary or in motion but only acts at a single point at any given time. The case of the brake pad is more complicated where there are various loads in different directions and the distributed friction force to be taken into account. To the best knowledge of the authors, this type of application is yet to be found in the available literature.

As mentioned earlier, the interaction of the friction pair is what leads to the vibration, this interaction occurs at the point of contact of the friction pair. The friction pair forms a non-conformal elastic contact [18]. This implies the contact patch between the friction pair may vary due to the motion of the pad and disc. The formation of small patches produces more noise than large contact patches and the size of the contact patches increase with brake pressure [19]. Another study also regarding contacts suggested that the rotation of the disc caused the shifting of the brake centre of pressure which increased the propensity of noise [20]. These contact patches are where the friction force is produced. This suggests that the friction force distribution is not evenly distributed along the contact points of the friction pair. The friction force plays another role in brake system vibration which is to act to bind the motion of the brake pad and brake disc during contact [21]. This is called the mode coupling phenomena.

This paper attempts to model the behaviour of the brake pad during braking with the focus placed on the brake pad motion from the model vibrations frequencies that arise during braking can be identified. All the obtained frequencies are vibrational characteristics of the brake pad, but not all will be relevant to audible noise as some may be a sensible vibration. It is up to the user's interest to which frequency range is relevant depending on the noise or vibration types analysed by the user.

METHODOLOGY

The friction pair modelling: Disc brake

The disc and pad act as a coupled system during braking; this causes the pad and disc to be excited and vibrate in a couple. The disc not only vibrates but also rotates at the same time. This brings to the assumption that the vibration of the disc acts as a travelling wave due to the rotation of the disc. The rotation of the disc, w_d is a rotational harmonic motion with amplitude, X and rotational frequency of w_1, where else, t is the time component of the equation.

$$w_d = X \cos w_1 \, t \tag{1}$$

The amplitude of mentioned motion in equation (1) is the vibration amplitude of the disc during rotation which is represented by equation (2). The disc vibrates at amplitude A at frequency, w_2. The disc carries certain number of the vibration waves, k which excites the brake pad at points, x along the length of the brake pad.

$$X = A \sin(kx - w_2 t) \tag{2}$$

The culmination of the disc rotation and the disc vibration leads to equation (3).

$$w_d = A \sin(kx - w_2 t) \cos w_1 \, t \tag{3}$$

The wave number, k is calculated using equation (4)

$$k = \frac{2\pi}{\lambda}, \tag{4}$$

where, λ is the wavelength. Equation (3) shows that the brake disc vibrational amplitude and its frequency must be known to compute the equation.

An experimental modal analysis (EMA) is performed on the brake disc to estimate these parameters. The EMA on the disc is conducted under free-free boundary condition. The EMA results are presented in Figure-1. The EMA frequency spectrum shows the frequencies and amplitudes which the brake disc is most likely to vibrate at given excitation. The higher the peak the more like it is to vibrate. Thus eight highest peaks frequency and amplitude are extracted from the EMA results for the computation of equation 3.

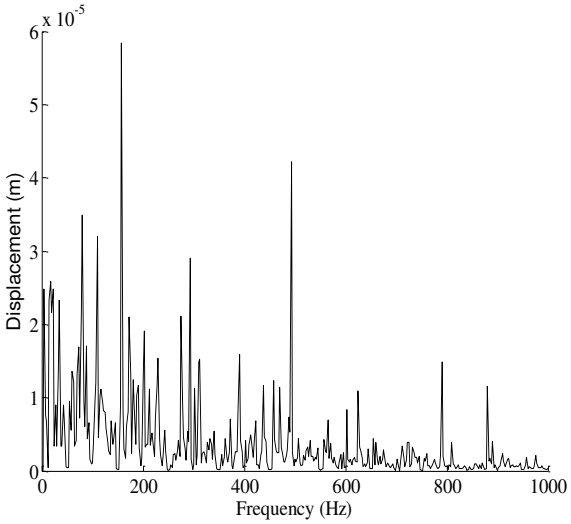

Figure-1. Experimental modal analysis of brake disc.

The extracted frequencies and amplitudes are shown in Table-1. The frequencies and amplitudes are numerically labelled with a prefix, *n* for ease of reference. Each frequency and amplitude pair will produce a sinusoidal wave and during actual running and braking operation all these waves superposition and acts as a single excitation. This behaviour is mathematically expressed in equation (5). This equation was computed with 4 different disc rotation frequencies R1 to R4. The rotational frequencies used in the simulation is shown in Table-2. The computation of equation (5) reveals the oscillation of the brake disc as a function of time. A fast Fourier transformation (FFT) is performed to identify the frequencies of the oscillation. From the FFT spectrum, peak frequencies are extracted and matched to the EMA frequencies.

Table-1. Frequencies and amplitude pairs from EMA resullts.

n	**Frequency** (Hz)	**Amplitude** (m)
1	157.5	5.85E-05
2	295.5	2.89E-05
3	390.0	1.59E-05
4	437.0	1.16E-05
5	492.5	4.22E-05
6	625.0	1.57E-05
7	790.0	1.49E-05
8	880.0	1.57E-05

Figure-2(a) to Figure-2(d) shows the timed oscillation of the brake disc and Figure-3(a) to Figure-3(d) shows the frequency spectrum of the oscillations for rotational frequencies R1 to R4 respectively. A combination of the frequency spectrum shown in Figure-3(a) to Figure-3(d) is made to show the effect of the increasing rotational frequency. By looking at Figure-4 the increase of the rotational speed caused the entire spectrum to shift to a higher frequency. This is a crucial observation, if the shifting of the frequency hits the resonance frequency of any brake system component, a high amplitude vibration would be produced.

During braking, rotational speed changes continuously, therefore momentarily a resonant frequency could be hit and vibration may be felt by the passenger. This may be one of the reasons for the intermittent behaviour of the brake system vibration.

$$\sum_{n=1}^{10} w_d = A_n \sin(k_n x - w_2 t) \cos w_1 \; t \qquad (5)$$

Table-2. Rotational frequencies used for computation.

	Rotational frequencies (rad/s)
R1	83.77
R2	104.72
R3	115.19
R4	125.66

The number of waves contained in the brake disc during vibration is half of the mode order of the frequency the disc is vibrating. The wavelength of these waves are dependent on the brake disc diameter which is 0.237 m. for example, at the 1st mode, the brake discs will contain half a wave, thus, that wavelength will be twice the diameter of the brake disc. The modes of the probable vibration, the number of waves and the corresponding wavenumber is shown in Table-3. These wavenumbers are incorporated in the equation (4) during the simulation.

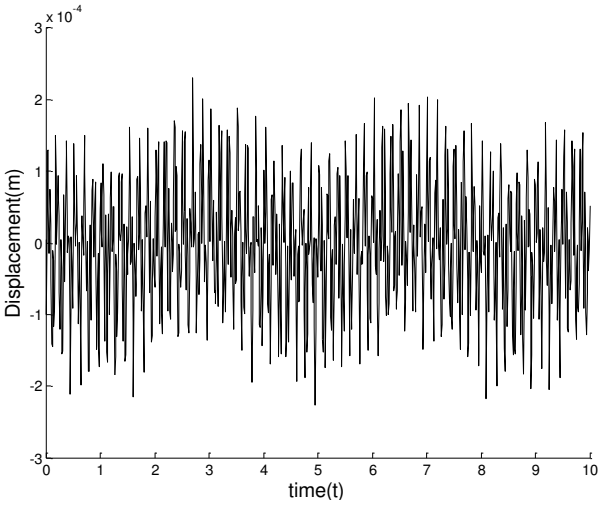

(a)

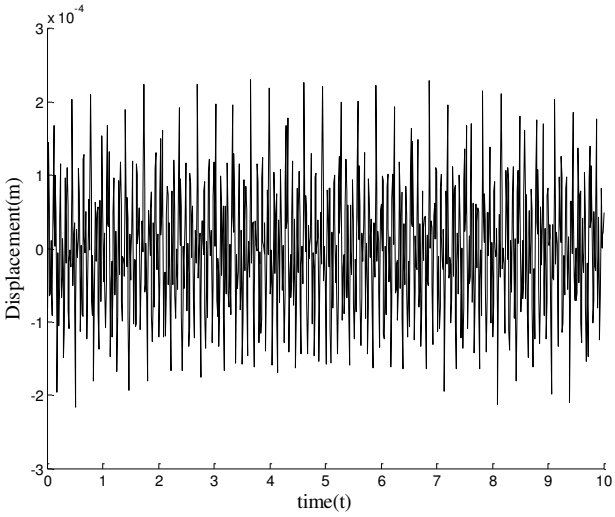

(b)

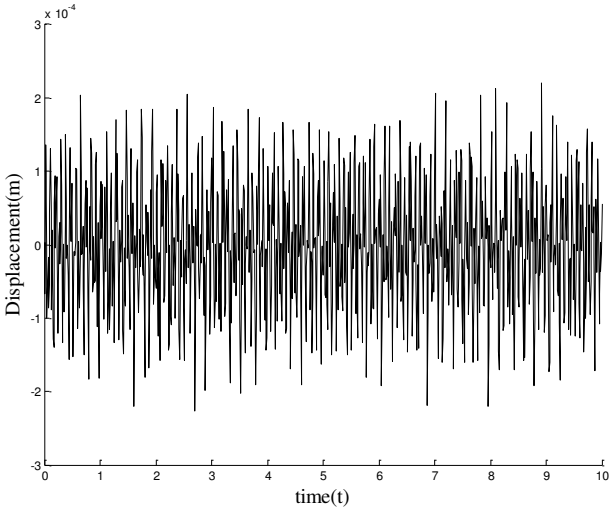

(c)

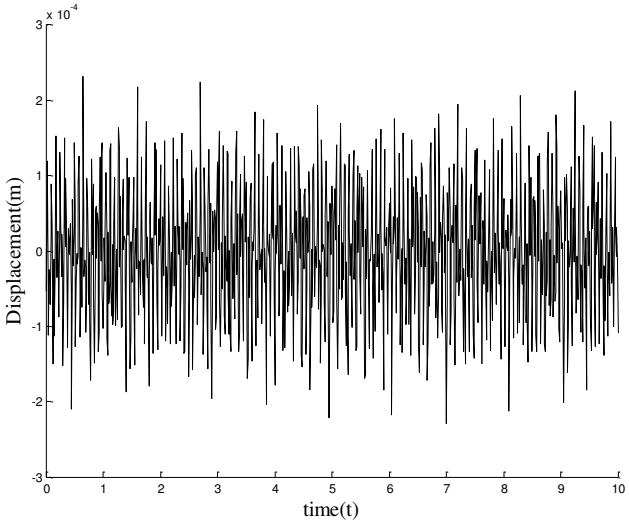

(d)

Figure-2. Brake disc oscillation for rotational frequency (a) R1 (b) R2 (c) R3 and (d) R4.

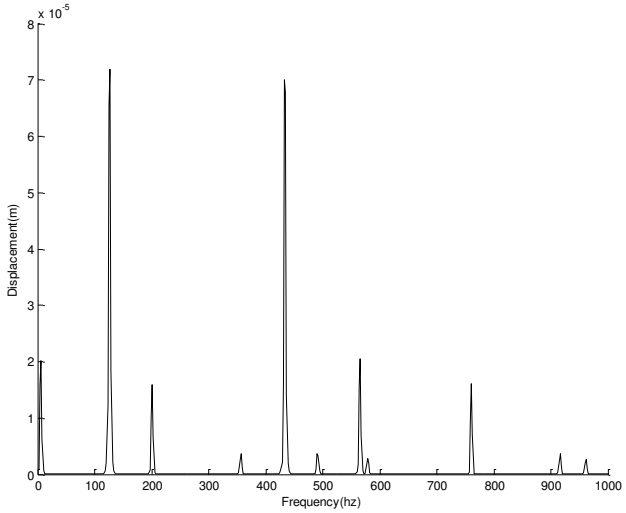

(a)

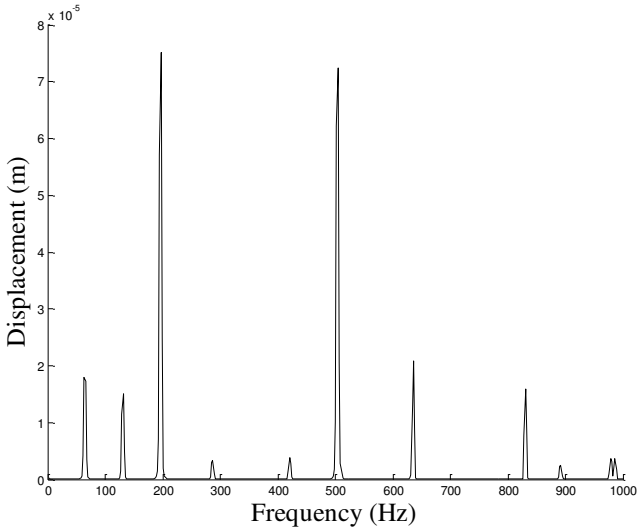

(b)

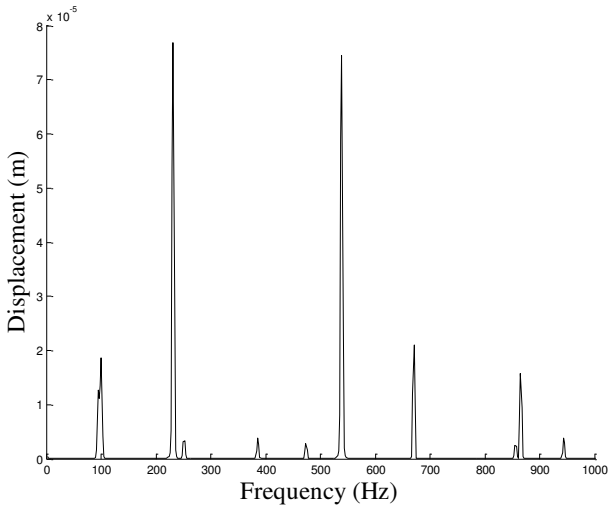

(c)

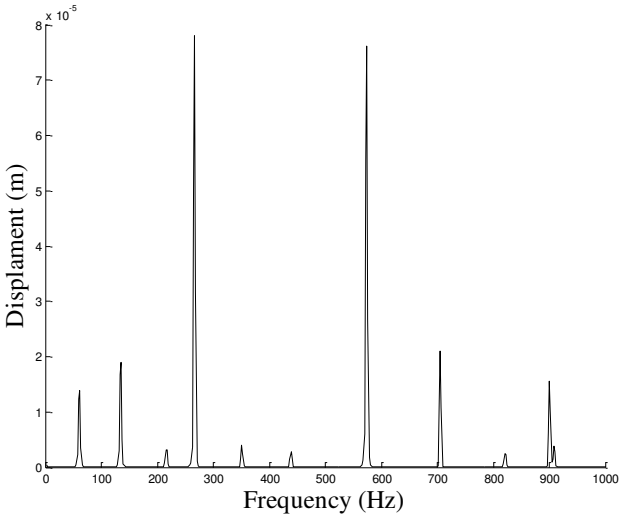

(d)

Figure-3. Frequency spectrum for rotational frequency (a) R1 (b) R2 (c) R3 and (d) R4.

The accuracy of each simulated frequency is calculated in reference to the EMA results. This is shown in Table-4. Again the frequencies are labelled numerically with a prefix, *n*. To show the accuracy visually, a plot is made. This plot is shown in Figure-5. It could be seen that the simulations are high in accuracy. Thus, the disc model may it be simple but it is sufficient enough to be used together with a brake pad model.

Table-3. Rotational frequencies used for computation.

N	Mode	Number of waves	Wavelength, λ	Wave number, K
1	1	0.5	0.47	13.25
2	3	1.5	0.15	39.77
3	5	2.5	0.09	66.28
4	6	3.0	0.07	79.54
5	7	3.5	0.06	92.80
6	8	4.0	0.05	106.05
7	9	4.5	0.05	119.31
8	10	5.0	0.04	132.57

Table-4. Accuracy calculation of simulated frequencies based on EMA frequencies.

	Extracted frequencies (Hz)				
n	**EMA**	**R1**	**R2**	**R3**	**R4**
1	157.5	127.14	131.25	120.48	133.30
2	295.5	220.99	211.87	231.73	215.33
3	390.0	354.78	285.05	383.49	348.66
4	437.0	432.71	420.41	471.68	436.81
5	492.5	488.06	504.49	539.35	574.21
6	625.0	566.01	635.74	670.60	705.46
7	790.0	760.84	830.56	865.43	799.80
8	880.0	955.66	885.93	943.35	900.29

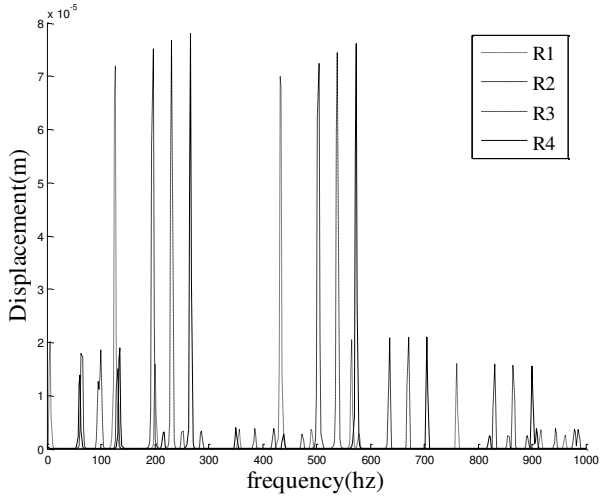

Figure-4. Combined frequency spectrum for all rotational frequency.

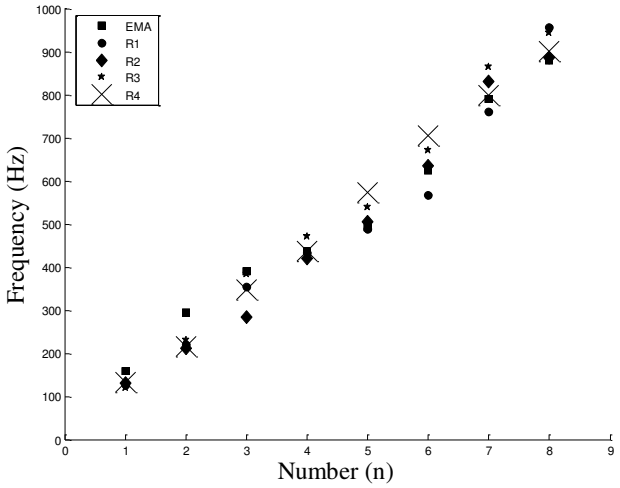

Figure-5. Accuracy plot of simulation and EMA.

The friction pair modelling: Brake pad

The brake pad mathematical modelling is done based on the friction pair diagrams shown in Figure-6. The forces mentioned earlier are derived and imposed on the brake pad. Referring to Figure-6, the piston imposes force on two points on the brake pad which is point x_a and x_b . The normal force, F_n, is expressed mathematically in equation (6) as a function of pressure, p, piston area, A_p and the delta Dirac function, δ which is to impose this force at specific points.

$$F_n = pA_p[\delta(x - x_a) + \delta(x - x_b)] \quad (6)$$

Next is the dynamic normal force, $F(x,t)$. This force is modeled by using the Hooke's law. During braking the pad experiances deformation due to the braking force and the motion of the disc. Equation (7) expresses this behaviour as the product of pad stiffness coeficient, k_p and the difference of disc motion, w_d and brake pad motion, w_b.

$$F(x,t) = k_p(w_d - w_b) \quad (7)$$

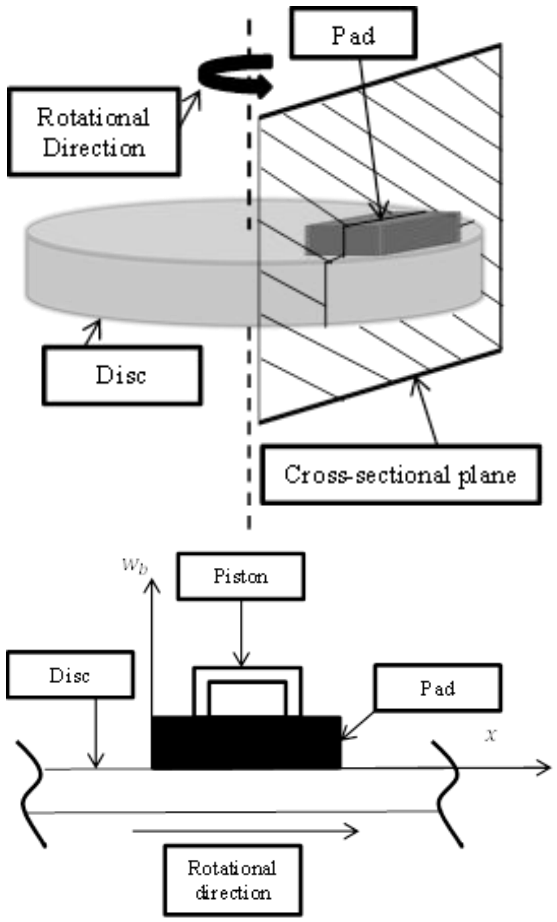

Figure-6. Schematic view of the friction pair used in modelling.

Assuming the disc and pad are always in contact, the Pasternak foundation model [22] is employed to add the shear force, F_s to the model. Equation (8) defines the shear force where K_G is the shear modulus of the brake pad.

$$F_s = -K_G \frac{\partial^2(w_d - w_b)}{\partial x^2} \quad (8)$$

From the dynamic normal force and the shear force, the damping could be defined. The damping force would the dynamic damping force, F_d and the shear damping force, F_{ds}. The damping would be the time derivative of the forces with the introduction of the damping constant, c_d, and shear damping constant, c_{ds}. This is shown in equation (9) and equation (10).

$$F_d = c_d \frac{\partial(w_d - w_b)}{\partial t} \quad (9)$$

$$F_{ds} = c_{ds} \frac{\partial^3(w_d - w_b)}{\partial t \partial x^2} \quad (10)$$

The friction force which acts along the contact point of the friction pair is the product of the brake pad friction coefficient and the total forces acting on the brake pad. The friction coefficient used in the simulation model is a constant of 0.35 which was obtained from the manufacturer of the actual brake system, that is also used in the present experiment.

To spread the friction force, F_f along the contact points of the brake pad the total force, F_T is integrated. The upper limit of this integral is the length of brake pad, L and the lower limit isthe arbitrary point, u.

$$F_f = -\mu \int_u^L F_T \, du \quad (11)$$

The brake pad is modelled as a beam, thus, the final equation is expressed in equation (12). The Euler-Bernoulli beam theory is adapted where the brake pad properties such as pad density, ρ, pad cross-section area, A_{cs}, pad young modulus, E, and pad moment of inertia, I.

$$\rho A_{cs} \frac{\partial^2 w_b}{\partial t^2} + EI \frac{\partial^4 w_b}{\partial x^4} = pA_p[\delta(x - x_a) + \delta(x - x_b)] + k_p(w_d - w_b) - K_G \frac{\partial^2(w_d - w_b)}{\partial x^2} + c_d \frac{\partial(w_d - w_b)}{\partial t} + c_{ds} \frac{\partial^3(w_d - w_b)}{\partial t \partial x^2} - \int_u^L F_T \, du \quad (12)$$

To solve equation 12, the dynamic green's equation is used. According to Dynamic Green formulation for the brake pad motion, w_b, can be expressed in equation 13 as a function of the green's function and forces acting on the brake pad. The green's function is then expressed in equation 14.

$$w_b = G(x,u)F_T \quad (13)$$

$$G(x,u) = \begin{cases} A_1 \cos qx + A_2 \sin qx \\ +A_3 \cosh qx + A_4 \sinh qx, \\ (0 \le x \le u) \\ B_1 \cos qx + B_2 \sin qx \\ +B_3 \cosh qx + B_4 \sinh qx, \\ (u \le x \le L) \end{cases} \quad (14)$$

The frequency parameter separation constant, q is derived from the Euler- Bernoulli beam equation which is expressed in equation (15).

$$\rho A_{cs} \frac{\partial^2 w_b}{\partial t^2} + EI \frac{\partial^4 w_b}{\partial x^4} = 0 \quad (15)$$

For normal mode oscillations, the brake pad can be expressed as a simple harmonic motion as in equation (16) where $X(x)$ the amplitude function is and w_n is the brake pad natural frequency.

$$w_b(x,t) = X(x) \cos w_n t \quad (16)$$

The second and fourth derivatives are substituted in equation (16) appropriately giving rise to equation (17). Rearranging the equation (17) enables the deployment of the general solution of the homogeneous equation for normal mode oscillations.

$$\rho A_{cs} X(x) w_n^2 + EI \frac{d^4 X(x)}{dx^4} = 0$$

$$q^4 X(x) + \frac{d^4 X(x)}{dx^4} = 0 \,,$$

where $q^4 = \frac{w^2 A_{cs}}{EI}$ (17)

The constants A_1 to A_4 and B_1 to B_4 is obtained by satisfying three conditions, first is the boundary conditions at the ends of the brake pad, second is the displacement, acceleration and moment continuity condition at $x = u$ and third is the shear force discontinuity at $x = u$. During braking the brake pad under goes bending motions [23], thus the boundary conditions at the end of the brake pads are free. This means that there is no bending moment and shear force at the free end. These are expressed mathematically in equation 18(a) to equation 18(d). The second order derivation with respect to x of the green's function in equation (14) is the bending moment where else the third derivative is the shear force.

$$G''(0,u) = 0 \quad (18a)$$

$$G''(L,u) = 0 \quad (18b)$$

$$G'''(0,u) = 0 \quad (18c)$$

$$G'''(L,u) = 0 \quad (18d)$$

The green function has two parts, one for the x-coordinates after and another for before the arbitrary point, u, but at the arbitrary point both part of the function must agree to each other in terms of displacement, acceleration and bending moment.

$$G(u^+,u) = G(u^-,u) \quad (19a)$$

$$G'(u^+,u) = G'(u^-,u) \quad (19b)$$

$$G''(u^+,u) = G''(u^-,u) \quad (19c)$$

The shear force is discontinuous with magnitude one at the arbitrary point for the green function.

$$EI[G'''(u^+,u) - G'''(u^-,u)] = 1 \quad (20)$$

The simulation is carried out in a closed-loop manner as can be seen in Figure-7. The forces acting on the brake pads are produced from the motion difference between the disc and pad.

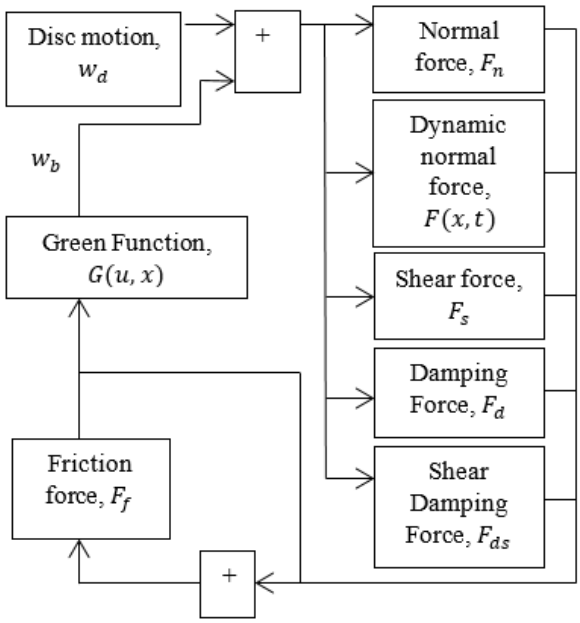

Figure-7. Simulation flows diagram.

These forces are incorporated into the green formulation to deduce the pad motion, w_b which in return is fed back in the loop. This is made as such so that the pad motion at any given time is influenced by the previous state of the system. Therefore, a continuous dynamic simulation close to real time system behaviour can be achieved. The brake dynamometer used to conduct the experimental testing to validate the simulation is shown in Figure-8.

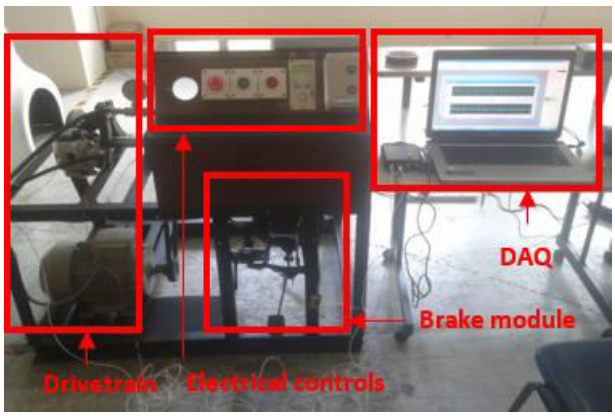

Figure-8. Overview of the brake dynamometer.

RESULTS AND DISCUSSIONS

The simulation directly will produce results for the brake pad motion from $x = 0$ to $x = L$ due to the forces acting at point, u. These results are super positioned from u_1 to u_{18} to create the reaction of distributed forces on the brake pad. The selected arbitrary point u is tabulated in Table-5 and the parameter used to simulate the model is shown in Table-6. As done with the brake disc results, the FFT is utilised to identify the frequencies of the vibration that occurred during operation.

Table-5. Selected arbitrary points for simulation.

u	Point position on x-axis
u_1	0
u_2	0.004
u_3	0.008
u_4	0.012
u_5	0.016
u_6	0.020
u_7	0.024
u_8	0.028
u_9	0.032
u_{10}	0.036
u_{11}	0.040
u_{12}	0.044
u_{13}	0.048
u_{14}	0.052
u_{15}	0.056
u_{16}	0.060
u_{17}	0.064
u_{18}	0.068

The FFT diagrams are shown for all the selected rotational speed in Figure-9(a) to Figure-9(d). These frequencies are compared to an experimental brake dynamometer results which are shown in Figure-10(a) to Figure-10(d). The error of the simulation frequencies comparing to the dynamometer experiment is calculated and tabulated in Table-7 and detail in Figure-11.

Table-6. Selected arbitrary points for simulation.

Constants	Value
Points where piston force is applied, x_a	0.023
Points where piston force is applied, x_b	0.053
Brake pressure (kPa)	90
Piston area (m^2)	0.025
Pad stiffness coeficient ($N/m/m^2$)	$0.18x10^{11}$
Pad damping constant (Ns/m)	1350
Length of brake pad (m)	0.068
Pad mass (kg)	0.8
Pad density (kgm^{-3})	2798
Pad cross-section area (m^2)	0.157
Pad young modulus (Pa)	$2.432x10^9$
Pad moment of inertia (m^4)	0.049
Friction coefficient	0.350

The simulation produces frequencies in a broad range. The frequency peaks from the simulation show harmonic behaviour. This is evident in Figure-9(a) to Figure-9(d). The harmonic pattern is closely related to the distributed friction force and the nature of the contact. The distributed friction force on the brake pad acts as an excitation force along the contact points of the friction fair. This means that the brake pad is being excited simultaneously along the contacting surface of the friction pairs. The simultaneous excitation coupled with the rotation of the disc produces the harmonics. Each point on the brake pad is excited by the friction force upon contact; the motion of the brake pad due to the excitation is transferred to the disc, this is called the mode coupling phenomena. Due to the rotation of the disc, this motion is transferred to the next point on the brake pad at the same time this point is already in an excited state due to the contact. This phenomenon occurs along the contact points continuously. Thus, the system gets more and more excitation energy and it's being excited continuously. This causes the brake pad to vibrate in a broad frequency harmonically.

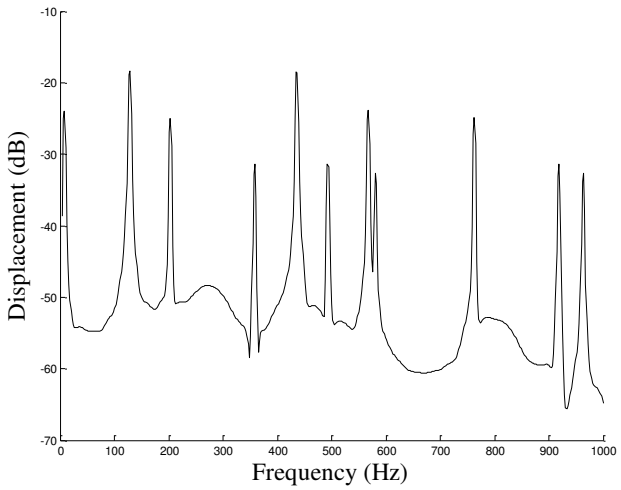

(a)

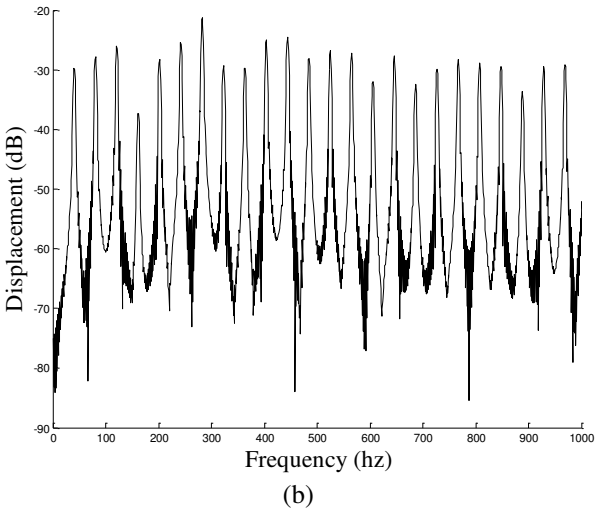

(b)

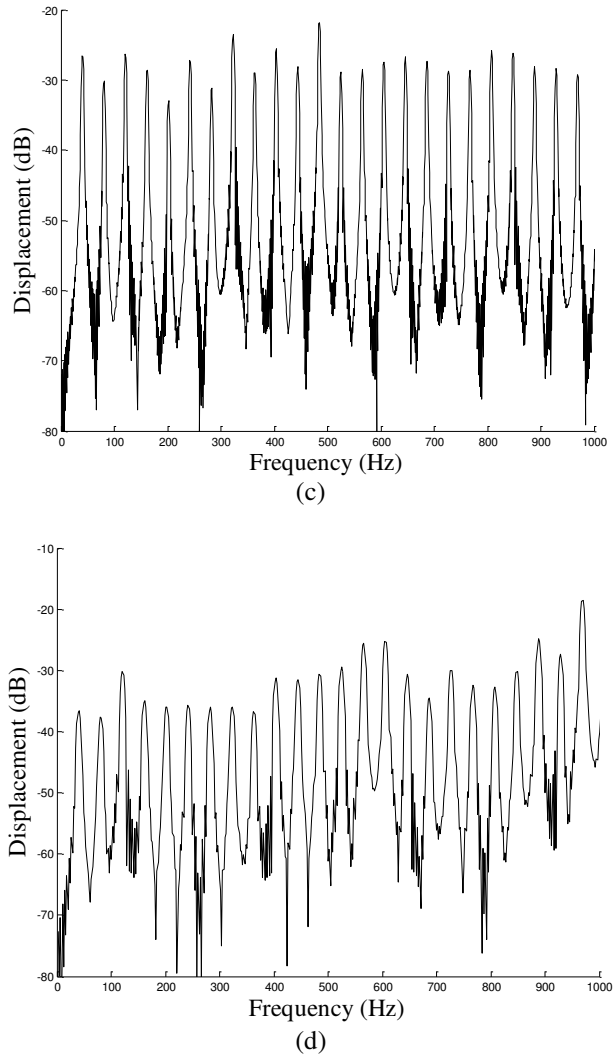

Figure-9. FFT plot for rotational frequency (a) R1, (b) R2, (c) R3 and (d) R4.

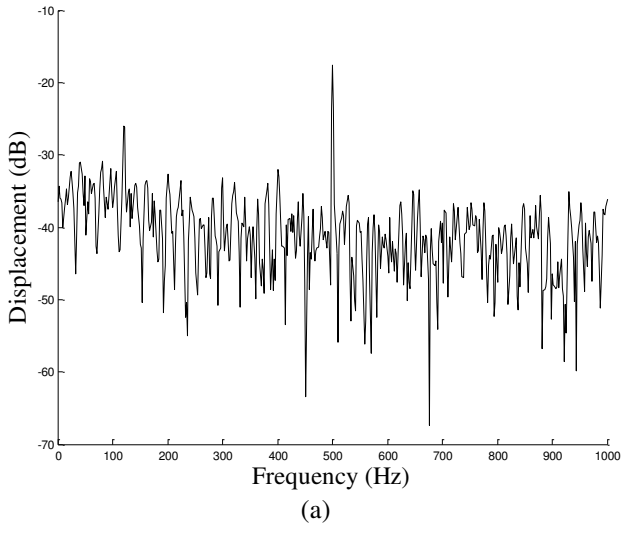

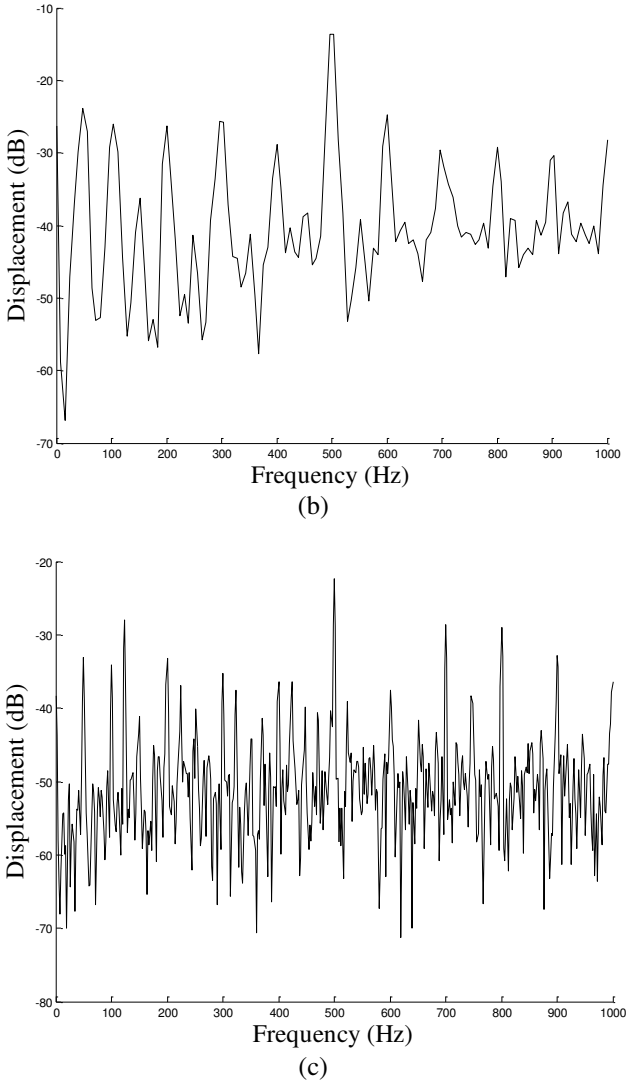

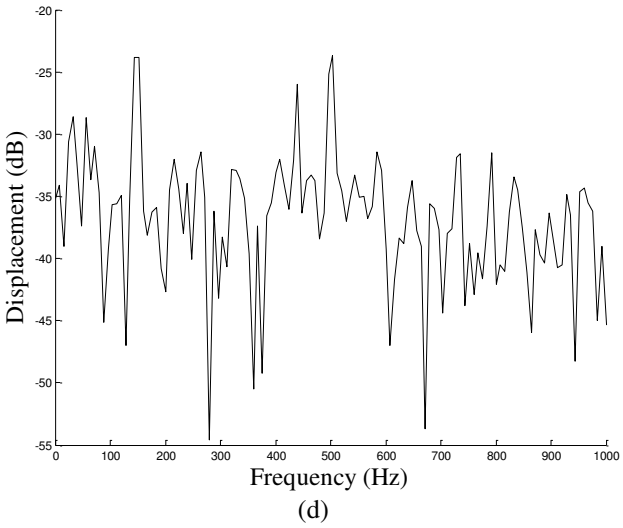

Figure-10. Dynamometer results for rotational speed (a) R1 (b) R2 (c) R3 (d) R4.

The results analysis shows that the simulation produced the brake pad vibration frequencies in high accuracy relative to the brake dynamometer results. This is evident in Figure-11. In average the simulation frequency differs about 5% from the experiment but for the rotational speed R1, a large deviation can be seen. The first prediction frequency is way off; the possible explanation is due to the intermittent nature of the brake vibration. A vibration at a certain frequency is not always noticeable all the time. The captured frequency from the experiment at that specific moment did not yield the frequency predicted by the model. Thus, the closest possible frequency was selected which comparatively resulted in a large error.

Even though all the other predictions are accurate, this inconsistency stresses the dynamic nature of the brake vibration, due to the dynamic characteristics of the normal force, all the other forces which are derived from this force behaves in a dynamic way. This dynamic interconnection brings a sense of randomness to the excitation force at any given time. This is the reason repeatability brake vibration measurements are difficult to produce. Here is where the derived model shows its capabilities by producing all the possible frequencies of which the vibration could occur. This can be seen especially in the rotational speed R4 where the experiment only yielded three noticeable frequencies but the modelling predicted a broad range of frequencies which is possible to occur at that speed. None the less the frequencies obtained from the experiment were simulated in high accuracy. Through experiment, only a few frequencies were observed, thus, the comparison was made with those visible frequencies to assess the model's prediction capabilities.

Predicting and identifying the vibration frequencies that occur in the brake system is the first step in reducing the brake system vibration. One of the methods is the usage of finite element model to extract eigenvalues to identify the natural frequency of the brake system at a specific time during operation. The next step is the parametric analysis to identify the propensity of the vibration and make necessary modification to eliminate the vibration.

Table-7. Experimental and simulation frequencies with its errors.

Speed	n	Experiment (Hz)	Prediction (Hz)	Error (%)
R1	1	40	6.152	84.62
	2	500	492.188	1.562
			Average	43.09
R2	1	48	38.964	18.82
	2	104	119.971	15.35
	3	144	160.986	11.79
	4	200	200.977	0.488
	5	232	241.992	4.306
	6	296	321.973	8.774
	7	336	361.963	7.727
	8	400	402.970	0.742
	9	432	442.969	2.539
	10	496	482.959	2.629
	11	696	684.961	1.586
	12	800	805.957	0.744
	13	896	886.963	1.008
			Average	5.886
R3	1	50	38.9684	22.06
	2	100	118.945	18.94
	3	150	159.961	6.640
	4	200	198.926	0.537
	5	224	239.941	7.116
	6	252	280.957	11.49
	7	300	319.922	6.640
	8	350	360.938	3.125
	9	400	401.953	0.488
	10	448	440.918	1.580
	11	470	481.934	2.539
	12	500	522.949	4.589
	13	524	563.965	7.626
	14	600	602.930	0.488
	15	652	643.945	1.235
	16	700	723.926	3.418
	17	746	764.941	2.539
	18	800	805.957	0.744
	19	900	885.938	1.562
			Average	5.310
R4	1	144	159.961	11.08
	2	440	442.969	0.674
	3	496	482.959	2.629
			Average	4.796

The modification in shape influences mass and the modification in material influences stiffness so that the natural frequency is shifted away from the targeted noise or vibration frequency. The proposed model in this paper simulates the motion of the brake pad during operation. Thus, the frequencies obtained are from vibrations that occur in real time as the simulation of the brake system operates. The simulation frequency spectrums show the vibration frequencies that occur during operation gives rise to harmonics with peak frequencies close to each other. Therefore, the attempt to shift the frequencies may lead to more problems than solutions. This is so because the

shifted frequency may fall on a peak frequency and cause severe resonating vibrations.

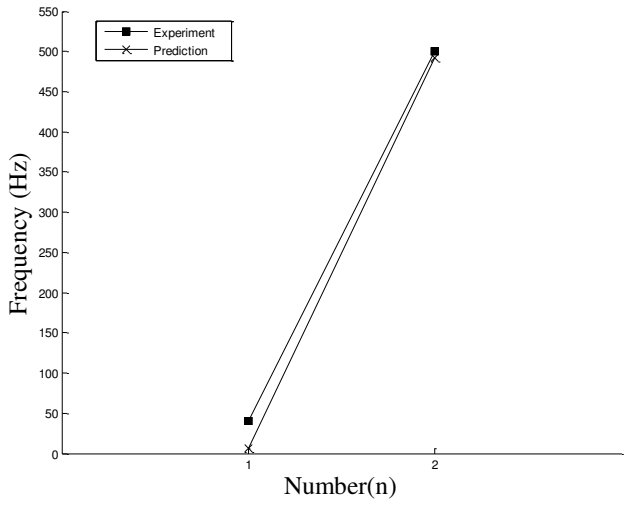

(a)

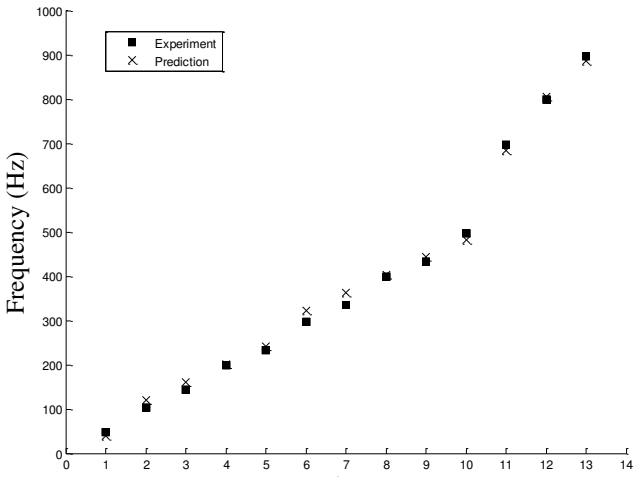

(b)

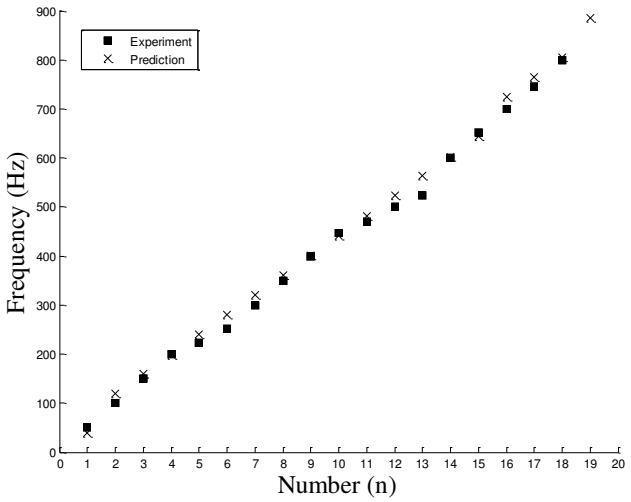

(c)

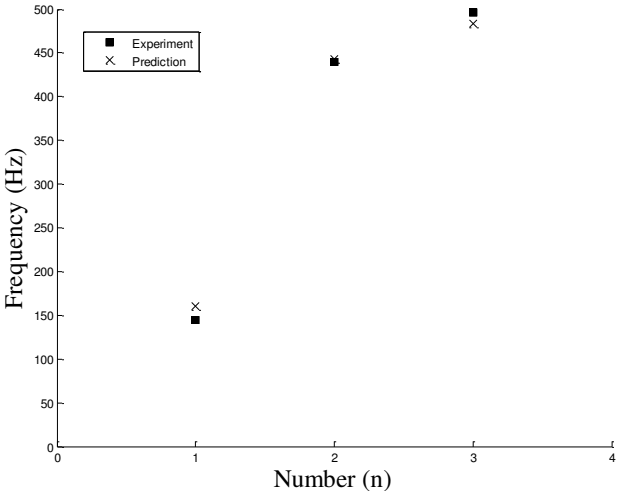

(d)

Figure-11. Accuracy comparison between simulation and experiment for speed (a) R1 (b) R2, (c) R3 and (d) R4.

At varying speeds, referring Figure-9 and Figure-10, it can be said that the passive attempts to eliminate brake vibration is very challenging, fine tuning of a brake system to perform quietly in a highly variable environment is close to impossible. Therefore, an active method in reducing brake noise is most likely the best suitable method. The active method such as actively controlling the normal force distributing which in turn control the friction force could be employed. In the venture to produce an active control of the normal force, this model could be used to predict the vibrations that occur before actual hardware implementation can be carried out.

The fundamental reason for the closely formed harmonic frequencies is the disc and pad contact itself. Having a non-contacting brake would eliminate the harmonics that arises due to the contact. One candidate for such a brake system is the Eddy Current Brake (ECB) which retards motion with magnetic fields. Even though the ECB concept has been around for quite some time but recently the boom of hybrid vehicles makes the ECB an interesting point. The weakness of the ECB is that it could not hold the brakes when the vehicle comes to a stop. Implementing the ECB as a fully functional brake in a hybrid vehicle braking system would greatly increase the regenerative capability of the vehicle coupled with regenerative braking which works with the same laws as the ECB. A fully functional ECB would remove the conventional friction brakes together with the noise and vibration problem that comes with it.

CONCLUSIONS

The model was able to simulate all the possible frequencies that might occur during braking operation. The simulated frequencies matched accurately with experimental brake dynamometer test results. The simulated frequencies are within the range of known noise and vibration frequencies such as groan, roughness, and judder. Even though the temperature is a major factor in brakes but in this paper, this factor is neglected but none

the less the validation is still expectable because during testing the brakes applied within a time period where there was no significant increase in temperature. With the validation of the model further studies using the model is possible. Testing could cover a wide range of braking parameters and also the dynamic behaviour at the brake pad and disc contacts. The model is still in its infancy and can be improved greatly.

The improvements can be made in terms of damping, the inclusion of temperature, wear and a more in-depth model of the brake disc. The damping equation used in the model is a simple one. A more complicated damping equation could be applied after performing detailed experiment on the brake pads to deduce its damping characteristics. Next is the temperature factor, it is well known that friction brakes produce heat during operation. The increase in temperature could contribute to the deformation of the brake pads thus the contact points could be compromised. A temperature function which is deduced from frictional contact could greatly improve results of brake pad deformation. Prolonged usages of the brakes lead to wear of the brake pad and disc. When a wear model is included in the current model, predictions of when the vibration hits a critical level could be made. Lastly, the disc could also be modelled in detail as was done with the brake pads and also with the recommendations made for the brake pad model could also be imposed on the brake disc. A complete friction pair model with the mentioned recommendation will become a powerful predictive tool.

ACKNOWLEDGEMENTS

The author, Muhammad Zahir Hassan, would like to express his gratitude and special acknowledgements to Universiti Teknikal Malaysia Melaka and Ministry of Higher Education Malaysia for the funding of the post-doctoral scholarship at the Department of Industrial Design, Eindhoven University of Technology, The Netherlands.

REFERENCE

[1] M.Z. Hassan, P.C. Brooks and D.C. Barton. 2008. Thermo-mechanical contact analysis of car disc brake squeal, Proceeding of 26th Annual SAE Brake Colloquium and Exhibition, 12-15 October 2008, San Antonio Texas, USA. SAE Technical Paper: 2008-01-2566.

[2] K. Magaswaran, A.S. Phuman Singh and M.Z. Hassan. 2013. An analytical model to identify brake system vibration within the low-frequency domain, Proceeding of 31st Annual SAE Brake Colloquium and Exhibition, 6-9 October 2013, Jacksonville Florida, USA. SAE Paper 2013-01-2033.

[3] Y.S. Lee. 1998. Frictional interface dynamics of an automotive disc brake, PhD Thesis, The University of Leeds, United Kingdom.

[4] H. Jacobsson. 2003. Aspects of disc brake judder, Proceedings of the Institution of Mechanical Engineers Part D: Journal of Automobile Engineering. 217(6): 419-430.

[5] B.A. Wernitz and N.P. Hoffmann. 2012. Recurrence analysis and phase space reconstruction of irregular vibration in friction brakes: Signatures of chaos in steady sliding, Journal of Sound and Vibration. 331(6): 3887-3896.

[6] M.Z. Hassan, P.C. Brooks and D.C. Barton. 2013. The evaluation of disc brake squeal propensity through a fully coupled transient thermomechanical model, Proceedings of the Institution of Mechanical Engineers, Part D: Journal of Automobile Engineering. 227(3): 361-375.

[7] A. Akay. 2002. Acoustics of friction. The Journal of the Acoustical Society of America. 111(4): 1525-1548.

[8] J. Kang, C.M. Krousgrill and F. Sadeghi. 2009. Wave pattern motion and stick–slip limit cycle oscillation of a disc brake, Journal of Sound and Vibration. 325(3): 552-564.

[9] K. Augsburg, H. Günther, H. Abendroth and B. Wernitz. 2003. Comparison between different investigation methods of quasi-static and dynamic brake pad behaviour, Proceeding of 21st Annual SAE Brake Colloquium and Exhibition, 6-8 October 2003, Hollywood Florida, USA. SAE Technical Paper: 2003-01-3340.

[10] E. Wegmann, A. Stenkamp and A. Dohle. 2009. Relation between Compressibility and Viscoelastic Material Properties of a Brake Pad, Proceeding of 27th Annual Brake Colloquium and Exhibition BRAKE 2009, 11-13 October 2009, Tampa Florida, USA.SAE Technical Paper: 2009-01-3017.

[11] M. Nishiwaki. 1993. Generalized theory of brake noise, Proceedings of the Institution of Mechanical Engineers Part D: Journal of Automobile Engineering, 207(3): 195-202.

[12] O. Giannini and A. Sestieri. 2006. Predictive model of squeal noise occurring on a laboratory brake, Journal of Sound and Vibration, 296(3), 583-601.

[13] R. Allgaier, L. Gaul, W. Keiper, K. Willner and N. Hoffmann. 2002. A study on brake squeal using a beam-on-disc model, Proceedings IMAC XX, 4-7 February 2002, Los Angeles, 1, 528-534, Society for Experimental Mechanics Inc., Bethel Connecticut, USA.

[14] Y.G. Joe, B.G. Cha, H.J. Sim, H.J. Lee and J.E. Oh. 2008. Analysis of disc brake instability due to friction-induced vibration using a distributed parameter model, International Journal of Automotive Technology, 9(2), 161-171.

[15] G.G.G. Lueschen, L.A. Bergman and D.M. McFarland. 1996. Green's functions for uniform Timoshenko beams, Journal of Sound and Vibration. 194(1): 93-102.

[16] M.A. Foda and Z. Abduljabbar. 1998. A dynamic green function formulation for the response of a beam structure to a moving mass. Journal of Sound and Vibration. 210(3): 295-306.

[17] M. Abu-Hilal. 2003. Forced vibration of Euler-Bernoulli beams by means of dynamic Green functions, Journal of Sound and Vibration. 267(2): 191-207.

[18] A.R. Abu Bakar, H. Ouyang and Q. Cao. 2003. Interface pressure distributions through structural modifications. Proceeding of 21st Annual SAE Brake Colloquium and Exhibition, 6-8 October 2003, Hollywood Florida, USA. SAE Technical Paper: 2003-01-3332.

[19] M. Eriksson, F. Bergman and S. Jacobson. 1999. Surface characterisation of brake pads after running under silent and squealing conditions, Wear. 232(2): 163-167.

[20] J.D. Fieldhouse and T.P. Newcomb. 1996. Double-pulsed holography used to investigate noisy brakes, Optics and Lasers in Engineering. 25(6): 455-494.

[21] N. Hoffmann, M. Fischer, R. Allgaier and L. Gaul. 2002. A minimal model for studying properties of the mode-coupling type instability in friction induced oscillations, Mechanics Research Communications. 29(4): 197-205.

[22] W.Q. Chen, C.F. Lü and Z.G. Bian. 2004. A mixed method for bending and free vibration of beams resting on a Pasternak elastic foundation, Applied Mathematical Modelling. 28(10): 877-890.

[23] J. D. Fieldhouse, N. Ashraf and C. J. Talbot. 2009. The measurement and analysis of the disc/pad interface dynamic centre of pressure and its influence on brake noise, SAE International Journal of Passenger Cars - Mechanical Systems. 1(1): 736-745.